

## Excited-State Reactions of Coumarins. VII. The Solvent-Dependent Fluorescence of 7-Hydroxycoumarins

Tetsuo MORIYA

Electrotechnical Laboratory, Umezono, Tsukuba, Ibaraki 305

(Received December 2, 1987)

The excited-state reactions of 7-hydroxycoumarin (7HC) and 7-hydroxy-4-methylcoumarin (7H4MC) have been studied by measuring the absorption and fluorescence spectra in aqueous and organic solvents under acidic and basic conditions. Based on the solvent-dependent fluorescence of the fluorophores, the solvents could be classified into several groups: hydroxylic solvents, nonhydroxylic solvents with low dielectric constants, and those with high dielectric constants. In the hydroxylic solvent, protonation, deprotonation, and tautomerization were the main reactions, while in the nonhydroxylic solvent the formation of hydrogen bonding and ion pairs was essential. The fluorescence in water-ethanol mixtures and in aqueous sodium dodecyl sulfate solutions has also been examined in relation to the solvent-dependent spectra in pure hydroxylic and nonhydroxylic solvents.

The complicated behavior of the fluorescence from 7-hydroxycoumarins has been extensively studied in organic solvents and in neutral, acidic, and basic aqueous solutions.<sup>1–4)</sup> Four fluorescent species have typically been observed in the photoexcited state, depending on the pH of the solution; they are identified as neutral, anionic, tautomeric, and protonated forms of the excited molecule. The reactions which generate these excited species are affected by the solvent so strongly that a careful examination of the fluorescence spectra, as well as the absorption spectra, is inevitable if we are to reach a correct conclusion. Basically, the solvents should be classified into two general groups in order to explain reasonably the fluorescent behavior of solvent-sensitive fluorophores; one group consists of “hydroxylic” solvents with hydroxyl substituents (–OH), and the other, of “nonhydroxylic” solvents without –OH. Such a classification is extremely meaningful, because the hydrogen-bonding ability and the ionizing power of the solvent determine in many ways the reaction process in excited states, such as the phototautomerization discussed in Ref. 4. As may readily be supposed, water, alcohols, water-organic mixtures, and aqueous solutions of surfactants belong to the hydroxylic-solvent group. Many of the aliphatic and aromatic solvents without –OH are nonhydroxylic solvents; the fluorescent behavior of the 7-hydroxycoumarins in these solvents is very different from that in the hydroxylic solvent. The purpose of the present study is to find a reasonable explanation of the solvent-dependent fluorescence by means of a unified model, one which includes the tautomerization, the acid-base reaction, and the ion pair formation with various additives.

### Experimental

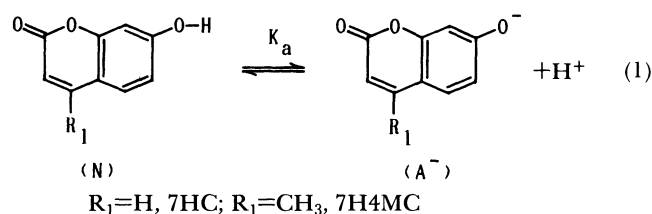
Commercial-grade reagents of 7-hydroxycoumarin (7HC, Wako Pure Chemical) and 7-hydroxy-4-methylcoumarin (7H4MC, Tokyo Kasei) were purified by recrystallization from ethanol and then washed with diethyl ether; 7HC, mp 234°C; 7H4MC, mp 186°C. The organic solvents were of a

spectroscopic grade from Dojindo Laboratories. The perchloric acid, hydrochloric acid, triethylamine (TEA), and butylamine (BA) were of a pure quality. The sodium dodecyl sulfate (SDS, Wako Pure Chemical) was of a biochemical grade. The water was permeated and distilled. The acidity and basicity of the solution were adjusted by the addition of HClO<sub>4</sub> and TEA (or BA) respectively.

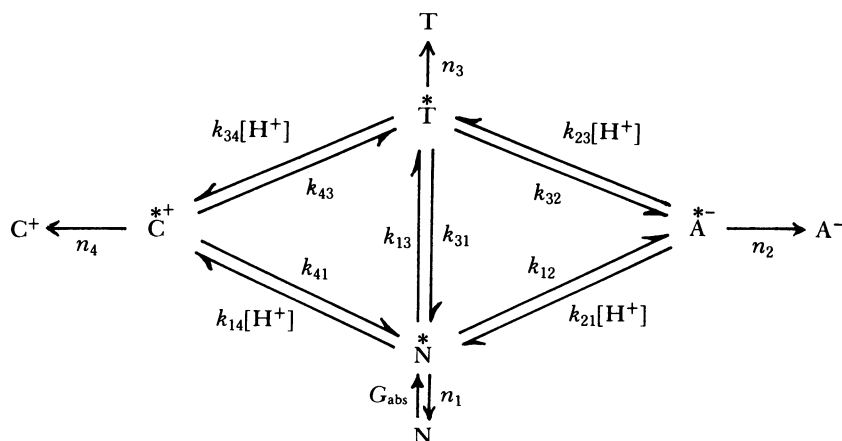
The UV absorption spectra were obtained on a Hitachi 323 spectrophotometer, while the fluorescence spectra were measured on a Hitachi MPF 4 spectrofluorometer with an S-5-type photomultiplier. The concentration of fluorescent molecules in the solutions was ca.  $4\text{--}5 \times 10^{-5}$  mol dm<sup>−3</sup>. Spectral measurements were performed at 20 or 25°C by controlling the temperature of the cell holder.

### Results and Discussion

**General Scheme for Excited-State Reactions.** In a previous study,<sup>4)</sup> the complex pH-dependence of the absorption and fluorescence spectra of 7HC and 7H4MC in aqueous solutions has been fully analyzed; the results may be summarized as follows. In the electronic ground state, there exist neutral molecular species (N) or anionic molecular species (A<sup>−</sup>), depending on the pH of the solution. If the pH is changed from neutral to basic, the molecule is deprotonated at the 7-hydroxyl group:



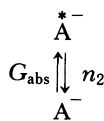
The absorption maxima of N and A<sup>−</sup> in the aqueous solutions were at 324 and 366 nm (7HC), and at 321 and 361 nm (7H4MC), respectively; 7HC, pK<sub>a</sub>=7.75; 7H4MC, pK<sub>a</sub>=7.84.<sup>5)</sup> Additionally, the absorption band corresponding to the cationic species (C<sup>+</sup>), protonated at the 2-carbonyl group, was found at 353 nm (7HC) and 345 nm (7H4MC) in concentrated sulfuric acid (H<sub>0</sub><−6).<sup>6)</sup> The absorption bands aligned in



Scheme 1.

wavelength as  $N < C^+ < A^-$ .

When N was optically excited at around its absorption-peak wavelength, the fluorescence from four molecular species in the excited state were observed with the variation in the pH. One was a usual neutral molecule ( $\dot{N}$ ), and another was a tautomeric molecule ( $\dot{T}$ ), in which a hydrogen of the 7-hydroxyl group was transferred to the 2-carbonyl group; contrary to the case of N,  $A^-$ , and  $C^+$ , the ground state of  $\dot{T}$  could never be found by absorption measurements. Analogously to the ground states, an excited cation ( $\dot{C}^+$ ) and an excited anion ( $\dot{A}^-$ ) were formed in strongly acidic solutions and in basic solutions respectively. A unified scheme for the excited-state reactions may be depicted as Scheme 1.<sup>4)</sup> Here,  $G_{abs}$  is the generation rate of  $\dot{N}$ , while the  $n_j$ 's are the transition rates of the excited species to their ground states. The  $k_{ij}$ 's and  $k_{ji}[H^+]$ 's are the protonation and deprotonation rates of the neutral, anionic, and cationic molecular forms in the excited state.  $k_{13}$  and  $k_{31}$  represent the reaction rates of the tautomerization that does not involve stepwise protonation or deprotonation processes, i.e., the "nondissociative" reaction rates.<sup>4,7)</sup> In aqueous solutions, the fluorescence-peak wavelengths of  $\dot{N}$ ,  $\dot{C}^+$ ,  $\dot{A}^-$ , and  $\dot{T}$  were 397, 431, 453, and 478 nm for 7HC, and 390, 419, 447, and 474 nm for 7H4MC, respectively. If  $A^-$  was selectively excited by choosing the wavelength in a neutral or basic solution, the situation became simple, because the fluorescent species was restricted to the anionic form ( $\dot{A}^-$ ) alone; this comes from the fact that  $\dot{A}^-$  is energetically most stable among the photoexcited states:<sup>4)</sup>



Scheme 2.

**Fluorescence Behavior in Hydroxylic Solvents.** As hydroxylic solvents, isobutyl alcohol (*i*-BuOH,  $D=18.3$ ), isopropyl alcohol (*i*-PrOH, 18.6), ethanol

(EtOH, 25.0), methanol (MeOH, 32.4), and water ( $H_2O$ , 80.4) were employed, where  $D$  represents the static dielectric constant of the solvents at 20 °C.<sup>8)</sup> The "acidic" and "basic" conditions have been realized by adding 0.29 mol dm<sup>-3</sup> HClO<sub>4</sub> and 0.22 mol dm<sup>-3</sup> TEA respectively to the solutions of 7HC and 7H4MC. The "strongly acidic" conditions have been attained by adding ca. 6 mol dm<sup>-3</sup> HClO<sub>4</sub>, and the "strongly basic" conditions, by adding TEA or BA up to ca. 4 mol dm<sup>-3</sup>. In order to visualize the fundamental aspect

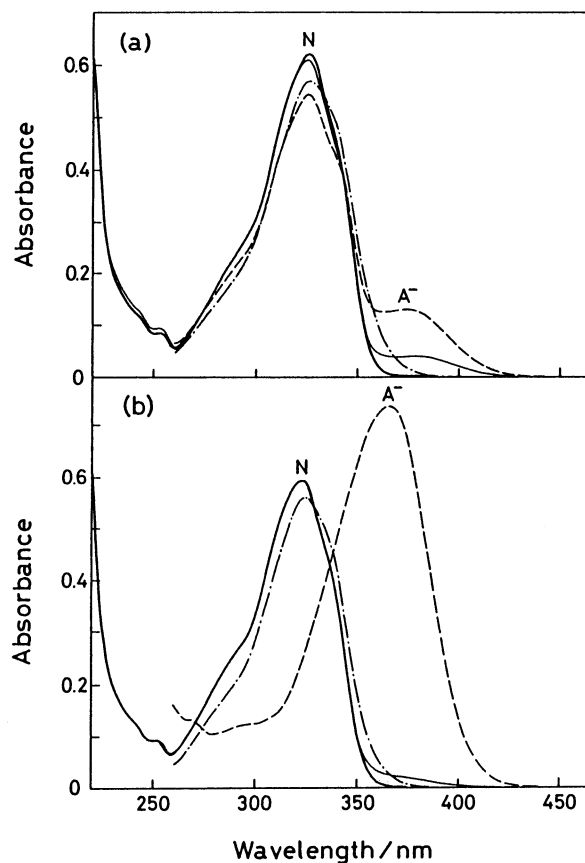


Fig. 1. UV absorption spectra of 7H4MC in *i*-BuOH (a) and in MeOH (b) for the neutral (—), acidic (---), strongly acidic (·····), and basic (-·-·-) solutions at 20 °C.

of electronically ground states, the absorption spectra of 7H4MC in *i*-BuOH are compared to those in MeOH in Fig. 1. Only the N absorption band is observable in the acidic *i*-BuOH and MeOH solutions, while  $C^+$  coexists with N in the strongly acidic solutions, as is shown by the shoulder on the long-wavelength side of the absorption spectra. The pure  $C^+$  state was ultimately reached in concd.  $H_2SO_4$  ( $D \approx 101$  at 25 °C) and was observed at ca. 345 nm. The  $A^-$  band is found as a shoulder around 375 nm in the neutral and basic *i*-BuOH and in the neutral MeOH. In the basic MeOH, on the other hand, the pure  $A^-$  absorption peaking at 365 nm is observed as a result of the dissociation of 7-OH. When the strongly basic condition was attained by the addition of up to 4 mol  $dm^{-3}$  of BA, the 7-OH group was completely dissociated, even in solvents less polar than MeOH. Since the molar extinction coefficients ( $\epsilon$ ) at the pure  $A^-$  absorption peak are thus measurable for all the hydroxylic solvents, the dissociation ratio of the fluorophore,  $[A^-]/([A^-]+[N])$ , at a given basicity of the solution can be evaluated by  $\epsilon^A/\epsilon_p^A$ , where  $\epsilon_p^A$  is the value for the pure  $A^-$  state, and  $\epsilon^A$ , for the  $A^-$  contribution under the present experimental conditions. Figure 2 presents the dependence of  $[A^-]/([A^-]+[N])$  on  $1/D$  in solutions containing 0.22 mol  $dm^{-3}$  of TEA. Based on the dissociation process of 7H4MC, the ionizing power of the hydroxylic solvents can be qualitatively estimated as  $H_2O \approx MeOH < EtOH < i\text{-}PrOH \approx i\text{-}BuOH$ . Irrespective of the drastic change in the ionizing power of the solvents, the spectral shape of each absorption band was similar in the solvents, whereas its peak was gradually blue-shifted with the increase in the  $D$  value (see Table 1).

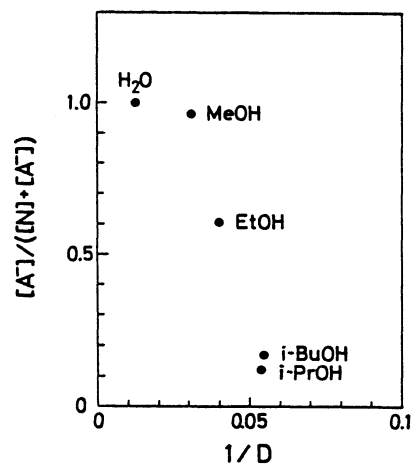


Fig. 2. Plots of the dissociation ratio,  $[A^-]/([A^-]+[N])$ , vs.  $1/D$  in the basic hydroxylic solvents with 0.22 mol  $dm^{-3}$  TEA.

Bearing the ground-state behavior in mind, the fluorescence spectra of 7H4MC in the neutral, acidic, strongly acidic, and basic solutions have been studied in detail; some typical spectra in MeOH are shown in Fig. 3. In spite of the complex behavior, the phenomena were common throughout the hydroxylic solvents, and either Scheme 1 or Scheme 2 was again applicable. When the light illumination was actuated at ca. 320 nm in the neutral, acidic, and strongly acidic solutions, Scheme 1 could be applied, for only the neutral excited species  $\dot{N}$  was generated by the light absorption; in contrast, when excitation was done at ca. 360 nm in the basic solution, Scheme 2 was applied. The peak wavelengths of the fluorescence bands

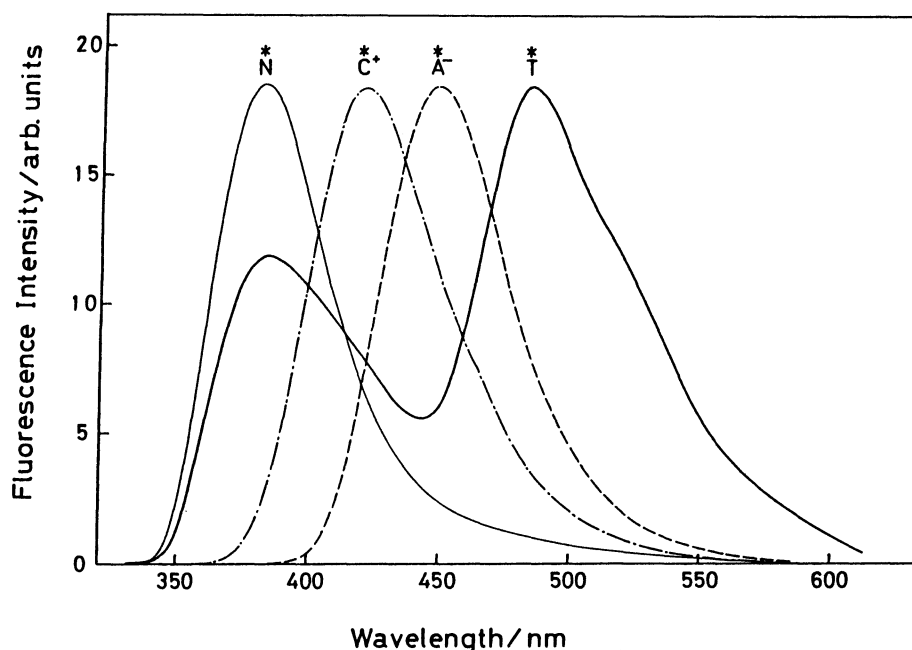


Fig. 3. Fluorescence spectra of 7H4MC in MeOH at 20 °C. The excitation wavelength was 320 nm for the neutral (—), acidic (— — —), and strongly acidic (---) solutions, and was 380 nm for the basic (— · —) solution.

Table 1. Peak Positions of the Absorption and Fluorescence Spectra of 7H4MC in the Hydroxylic Solvents under Neutral, Acidic, and Basic Conditions at 20 °C

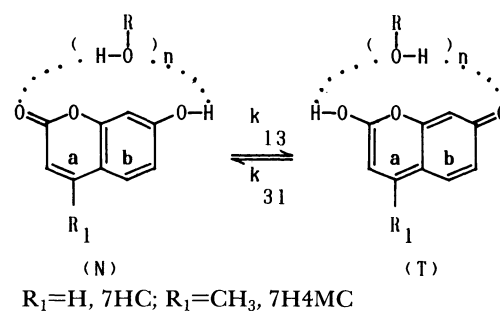
| Solvent          | $D^{20}$ | Absorption |                   |                | Fluorescence          |                    |                    |                   |
|------------------|----------|------------|-------------------|----------------|-----------------------|--------------------|--------------------|-------------------|
|                  |          | N          | C <sup>+</sup> a) | A <sup>-</sup> | $\tilde{N}^{*b)}$     | $\tilde{C}^{*+b)}$ | $\tilde{A}^{*-c)}$ | $\tilde{T}^{*b)}$ |
| <i>i</i> -BuOH   | 17.1     | 326        | (345)             | 375            | 380                   | 419                | 446                | 485               |
| <i>i</i> -PrOH   | 18.3     | 325        | (345)             | 375            | 379                   | 419                | 446                | 486               |
| EtOH             | 24.2     | 324        | (345)             | 373            | 380                   | 420                | 448                | 486               |
| MeOH             | 32.6     | 323        | (345)             | 365            | 382                   | 420                | 448                | 484               |
| H <sub>2</sub> O | 78.5     | 321        | (345)             | 361            | ca. 385 <sup>d)</sup> | 421                | 446                | 476               |

a) The value obtained in concd. H<sub>2</sub>SO<sub>4</sub>. b) Found by excitation at 320 nm. c) Found by excitation at 380 nm. d) Observed only as a shoulder around 385 nm.

thus obtained were in this order:  $\tilde{N}^{*} < \tilde{C}^{*+} < \tilde{A}^{*-} < \tilde{T}^{*}$ ; this order is parallel with that in the ground state except for  $\tilde{T}^{*}$ . Table 1 gives the peak position of each absorption and fluorescence band observed in the hydroxylic solvents. As  $D$  is increased from *i*-BuOH to H<sub>2</sub>O, the  $\tilde{T}^{*}$  band obviously blue-shifts, while the other three bands show small shifts without any systematic tendency. The optical transitions of coumarins originate from the  $\pi$ - $\pi^{*}$  transition, which induces a very strong absorption ( $\epsilon > 10^4$  cm<sup>-1</sup> mol<sup>-1</sup> cm<sup>3</sup>).<sup>9)</sup> If there is no other solvent-solute interaction than the dielectric effect due to the molecular polarization, the dipole moment of the excited  $\pi$ -state ( $\mu_e$ ) is usually larger than that of the ground state ( $\mu_g$ ); then, the fluorescence band is red-shifted with the increase in the solvent polarity, whereas the polarity effect on the absorption band is small.<sup>10)</sup> Adopting the qualitative parallelism of solvent polarity with  $D$ , the shifts of the absorption and fluorescence bands of the neutral and anionic species contradict the above-mentioned presumption ( $\mu_e > \mu_g$ ) for the  $\pi$ -electron system. Probably, the hydrogen bond between the fluorophore and the solvent molecule as a result of the atomic-level interaction, which originates from the difference in the electronegativity of the heteroatoms, must be appropriately taken into account in the case of 7-hydroxycoumarins. The hydrogen-bonding interaction will stabilize the  $\pi$ -electron system by spreading its distribution towards nearby solvents. If the stabilization is more prominent in the ground state than in the excited state, the data for the neutral and anionic species, which suggest a more polar structure in the ground state ( $\mu_e < \mu_g$ ), are consistently explained. It is hard to conjecture the electronic structures of the cationic and tautomeric species from the data in Table 1, for the pure absorption of the former is not found except in concd. H<sub>2</sub>SO<sub>4</sub>, while that of the latter cannot be found under any usual conditions. Nevertheless, based on the relative energy position and the small shift of the fluorescence band,  $\tilde{C}^{*+}$  seems to belong in the same groups as  $\tilde{N}^{*}$  and  $\tilde{A}^{*-}$ . The tautomeric species, on the other hand, must have a special  $\pi$ -electron distribution compared with the other three, because the increase in the hydrogen-bonding ability or the solvent polarity destabilized the excited state. Since the T absorption

does not appear, the energy position of T may be highly pulled up from those of N and A<sup>-</sup>. The chemical aspect of the tautomer can be partly presumed from its strained molecular structure, including a quinoid structure of the b ring of T in Scheme 3 as the main resonance component.

The  $\tilde{C}^{*+}$  and  $\tilde{A}^{*-}$  bands were singly observed in the strongly acidic and basic solutions respectively, while the  $\tilde{N}^{*}$  and  $\tilde{T}^{*}$  bands are always observed in pairs. An especially interesting situation occurs in the acidic solutions with 0.2–0.5 mol dm<sup>-3</sup> HClO<sub>4</sub>, where the rapid equilibration between  $\tilde{N}^{*}$  and  $\tilde{T}^{*}$  seems to be realized after the excitation of N; spectroscopically, the fluorescence of  $\tilde{N}^{*}$  and tautomeric  $\tilde{T}^{*}$  species is clearly measured, but neither that of  $\tilde{C}^{*+}$  nor that of  $\tilde{A}^{*-}$  is (see Fig. 3). It has been shown in Ref. 4 that the tautomerization of  $\tilde{N}^{*}$  to  $\tilde{T}^{*}$  is promoted by dissociative and nondissociative processes. The dissociative process has two possible pathways. The one generates the intermediate protonated species as  $\tilde{N}^{*} \rightarrow \tilde{C}^{*+} \rightarrow \tilde{T}^{*}$ ; the other generates the intermediate deprotonated species as  $\tilde{N}^{*} \rightarrow \tilde{A}^{*-} \rightarrow \tilde{T}^{*}$ . The absence of  $\tilde{C}^{*+}$  and  $\tilde{A}^{*-}$  in the fluorescence spectra does not mean that  $\tilde{C}^{*+}$  and  $\tilde{A}^{*-}$  are not generated, but that the reactions rapidly proceed toward  $\tilde{T}^{*}$  without enough time to fluoresce in the  $\tilde{C}^{*+}$  or  $\tilde{A}^{*-}$  state, as will be discussed further later. In hydroxylic solvents, there is another possibility: that  $\tilde{N}^{*}$  is directly converted to  $\tilde{T}^{*}$  by means of the concerted transfer of a hydrogen from the hydroxyl site to the carbonyl site with the aid of hydrogen bonds of solvent molecules described as:



Scheme 3.

The same discussion holds for the three reversed reaction pathways from  $\tilde{T}^{*}$  to  $\tilde{N}^{*}$ . Except for the conditions

of  $[\text{HClO}_4] = 0.2\text{--}0.5 \text{ mol dm}^{-3}$ , the fluorescence of  $\tilde{\text{A}}^*$  or  $\tilde{\text{C}}^*$  has been more or less observed in the wavelength region between the  $\tilde{\text{N}}$  and  $\tilde{\text{T}}$  bands. By chance, in the 7HC and 7H4MC solutions with  $[\text{HClO}_4]$  of  $0.29 \text{ mol dm}^{-3}$  the fluorescence from  $\tilde{\text{A}}^*$  and  $\tilde{\text{C}}^*$  is simultaneously negligible; such peculiar conditions were helpful in the detailed study of tautomerization reactions in aqueous solutions.<sup>4,11)</sup> Since the  $\tilde{\text{N}}$  and  $\tilde{\text{T}}$  bands are separated enough in wavelength, and since their spectral shapes are almost entirely maintained throughout the solvents, the fluorescent yields of  $\tilde{\text{N}}$  and  $\tilde{\text{T}}$  may be rigorously compared with each other. Although the  $D$  value is used as a convenient parameter to describe the macroscopic properties of solvents, it is not an appropriate measure of solvent-solute or solute-solute interactions. Therefore, the ratio of the fluorescence intensity of  $\tilde{\text{T}}$  to that of  $\tilde{\text{N}}$ ,  $I^{\text{T}}/I^{\text{N}}$ , is plotted in Fig. 4 against the polarity factor,  $(D-1)/(2D+1)$ ; the factor was first derived by Kirkwood<sup>12)</sup> to estimate the activity coefficient of reacting molecules in solvents and was then discussed extensively by Winstein et al.<sup>13)</sup> in treating the linear free-energy relationship for the solvolysis rate of *t*-butyl chloride. As  $I^{\text{T}}/I^{\text{N}}$  is the value that reflects the tautomerization reaction rate in the solvents, the correlation between  $\log(I^{\text{T}}/I^{\text{N}})$  and  $(D-1)/(2D+1)$  was examined first; however, the plots showed a marked curvature (Fig. 4). It is frequently seen that  $(D-1)/(2D+1)$  does not fully correlate with the log of the reaction rate measured. Böhme et al.<sup>14)</sup> plotted, though the theoretical basis was rather poor, the log of the hydrolysis rate of halogenated compounds against "log  $D$ "; they thus obtained a quite straight relationship. Therefore, this type of plot has been applied to the present problem, as is shown in Fig. 5; the plots are widely fitted with  $I^{\text{T}}/I^{\text{N}} \propto D^{2.0 \pm 0.05}$  for 7H4MC and with  $\propto D^{1.7 \pm 0.05}$  for 7HC at  $20^\circ\text{C}$ . This

empirical relation is exciting, because many reaction rates, either dependent on or independent of  $D$ , must be practically concerned in each fluorescence process.

In case that no fluorescence of  $\tilde{\text{A}}^*$  and  $\tilde{\text{C}}^*$  is detected, the following inequalities are satisfied:<sup>11)</sup>

$$k_{12}, k_{32} \ll k_{21}[\text{H}^+], k_{23}[\text{H}^+],$$

and

$$k_{14}[\text{H}^+], k_{34}[\text{H}^+] \ll k_{41}, k_{43}. \quad (2)$$

Experimentally, all decay rates of the excited species,  $n_i$ 's, are of the same order;<sup>4,11)</sup> the integrated spectral intensity of each absorption band shows so little change with altering the solvents that the radiative-decay probabilities of the excited species ( $n_i^r$ ) are nearly constant;<sup>10)</sup> the decay rates  $n_i$ 's are rather insensitive to  $D$ , judging from the fluorescence-yield and the lifetime measurements.<sup>4,11)</sup> Based on these clues, we obtain the following theoretical prediction by analyzing the rate equations given in Ref. 4:<sup>11)</sup>

$$\frac{I^{\text{T}}}{I^{\text{N}}} \propto \frac{n_3^r}{n_1^r} \cdot \frac{k_{13} + k_{13}^{\text{A}} + k_{13}^{\text{C}}}{n_3 + k_{31} + k_{31}^{\text{A}} + k_{31}^{\text{C}}}, \quad (3)$$

where, corresponding to the forth- and back-reaction pathways of  $\tilde{\text{N}} \rightleftharpoons \tilde{\text{A}}^* \rightleftharpoons \tilde{\text{T}}$ :

$$k_{13}^{\text{A}} = k_{12} \cdot \frac{k_{23}[\text{H}^+]}{n_2 + k_{21}[\text{H}^+] + k_{23}[\text{H}^+]},$$

$$k_{31}^{\text{A}} = k_{32} \cdot \frac{k_{21}[\text{H}^+]}{n_2 + k_{21}[\text{H}^+] + k_{23}[\text{H}^+]}, \quad (4)$$

and corresponding to the pathways of  $\tilde{\text{N}} \rightleftharpoons \tilde{\text{C}}^* \rightleftharpoons \tilde{\text{T}}$ :

$$k_{13}^{\text{C}} = k_{14}[\text{H}^+] \cdot \frac{k_{43}}{n_4 + k_{41} + k_{43}},$$

$$k_{31}^{\text{C}} = k_{34}[\text{H}^+] \cdot \frac{k_{41}}{n_4 + k_{41} + k_{43}}. \quad (5)$$

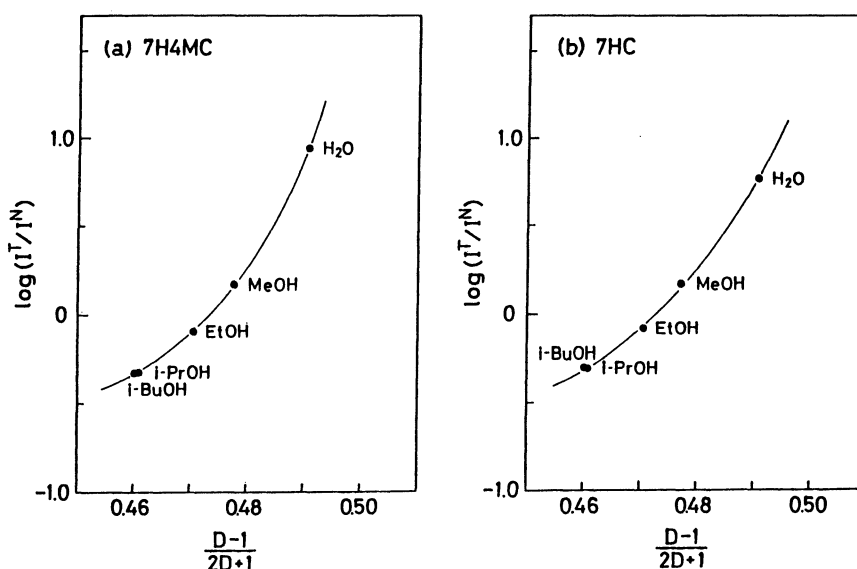


Fig. 4. Plots of  $\log(I^{\text{T}}/I^{\text{N}})$  vs.  $(D-1)/(2D+1)$  in the acidic hydroxylic solutions of 7H4MC (a) and of 7HC (b) at  $20^\circ\text{C}$ .

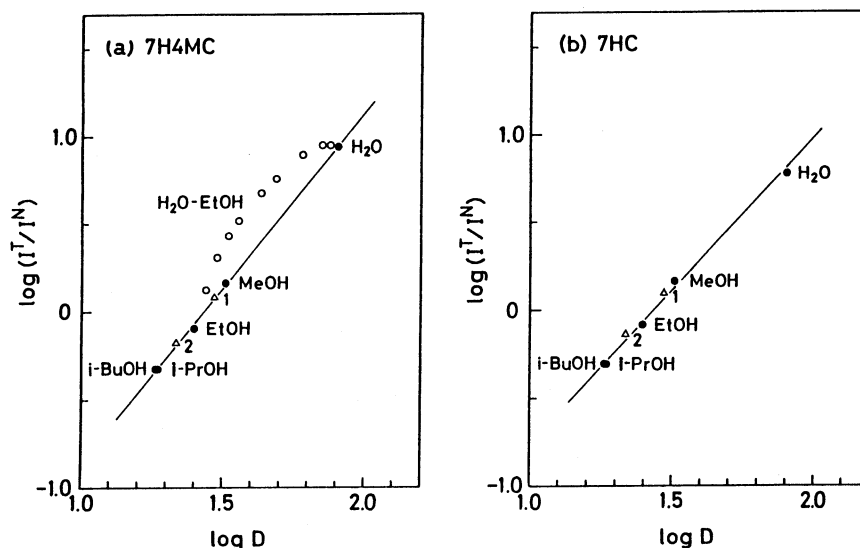


Fig. 5. Plots of  $\log(I^T/I^N)$  vs.  $\log D$  in the acidic hydroxylic solutions of 7H4MC (a) and of 7HC (b) at 20°C. The plots for the MeOH-EtOH mixture (1), for the EtOH-*i*-PrOH mixture (2), and for the H<sub>2</sub>O-EtOH mixture (O) are also shown.

Although the  $D$  dependency of the  $n_3$ ,  $k_{13}$ 's, and  $k_{31}$ 's in Eq. 3 has not yet been exactly ascertained, it can be asserted that at least one of the tautomerization rates  $k_{13}$ ,  $k_{13}^A$ , or  $k_{13}^C$ , would have a term superlinearly dependent on  $D$  if their power expansions of  $D$  could be carried out. The reaction pathway described by  $k_{13}$  in Scheme 3 is, of course, promoted by the increase in  $D$ , for the bridge of hydrogen bonds transferring a hydrogen between the two reactive sites is readily enhanced in polar hydroxylic solvents. This prediction will be confirmed later by an experiment in mixed solvents with various amounts of H<sub>2</sub>O.

As for the dissociative tautomerization pathways in an acidic solution, the contribution from  $k_{13}^C$  is more important than that  $k_{13}^A$ . Equations 4 and 5 show that  $k_{13}^C$  linearly increases depending on  $[H^+]$ , but that  $k_{13}^A$  saturates at a large  $[H^+]$  value. Furthermore, under the acidic conditions employed, the transiently generated  $C^+$  is really evidenced by means of the fluorescence quenching measurement due to halide ions, as will be discussed in a later section. Therefore,  $k_{13}^C \gg k_{13}^A$  is reasonable, and the dependence of  $I^T/I^N$  on  $D$  in Fig. 5 is mainly determined by the competition of  $k_{13}$  and  $k_{13}^C$ . The back-reaction rates,  $k_{31}$  and  $k_{31}^C$ , cannot dominate the  $D$  dependence of  $I^T/I^N$ , because these rates must compete with the large decaying probability,  $n_3$  (ca.  $2 \times 10^8 \text{ s}^{-1}$ ),<sup>4)</sup> in the denominator of Eq. 3, which is only slightly dependent on the  $D$  value.

Since, at any rate, the straight relationship in Fig. 5 holds very widely from *i*-BuOH to H<sub>2</sub>O,  $\log D$  for various hydroxylic solvents can be employed in order to estimate the chemical properties of microenvironments, such as the microscopic polarity and the hydrogen-bonding ability. It has been further revealed that the data in the mixed solvents of MeOH-EtOH

and EtOH-*i*-PrOH follow well the predicted relation; the representative points are plotted in Fig. 5. Therefore,  $\log D$  is the generally usable parameter that describes the microenvironment and the solvent-solute interaction, even in such mixed solvents.

#### Fluorescence Behavior in Nonhydroxylic Solvents.

As compared with the hydroxylic solvents, nonhydroxylic solvents (also called "inert" or "aprotic" solvents) have so little hydrogen-bonding ability by themselves that the situation for excited-state reactions, as well as for ground-state equilibria, becomes extremely altered. Moreover, the formation of hydrogen bonds and ion pairs between acids and bases in the solution must be taken into account as important phenomena, for the dissociation process of proton liberation is highly suppressed in nonhydroxylic solvents due to the large or immeasurable "autoprotolysis" constant (for acetonitrile,  $pK_{HS} \approx 28.5$  at 25°C, while it is immeasurable for the others).<sup>15)</sup> As nonhydroxylic solvents, dioxane ( $D=2.2$  at 20°C), benzene (2.3), chloroform (4.8), ethyl acetate (6.2), dichloromethane (7.4), acetone (21.1), and acetonitrile (36.8) were examined; these solvents were afterwards classified into three groups (1, 2a, and 2b), as indicated in Table 2, in order to make the subsequent discussion systematic. The "acidic" and "basic" conditions have been realized, as before, by the addition of  $0.29 \text{ mol dm}^{-3}$  of HClO<sub>4</sub> and  $0.22 \text{ mol dm}^{-3}$  of TEA respectively. Since benzene, CHCl<sub>3</sub>, and CH<sub>2</sub>Cl<sub>2</sub> could not dissolve the indicated amount of HClO<sub>4</sub>, the data in these solvents under the acidic conditions were taken into account as references.

The typical absorption spectra of 7H4MC in dioxane and in CH<sub>3</sub>CN are shown in Fig. 6. In the acidic and basic dioxane, the absorption peak was red-shifted from that in the neutral solution (Fig. 6(a)). The same

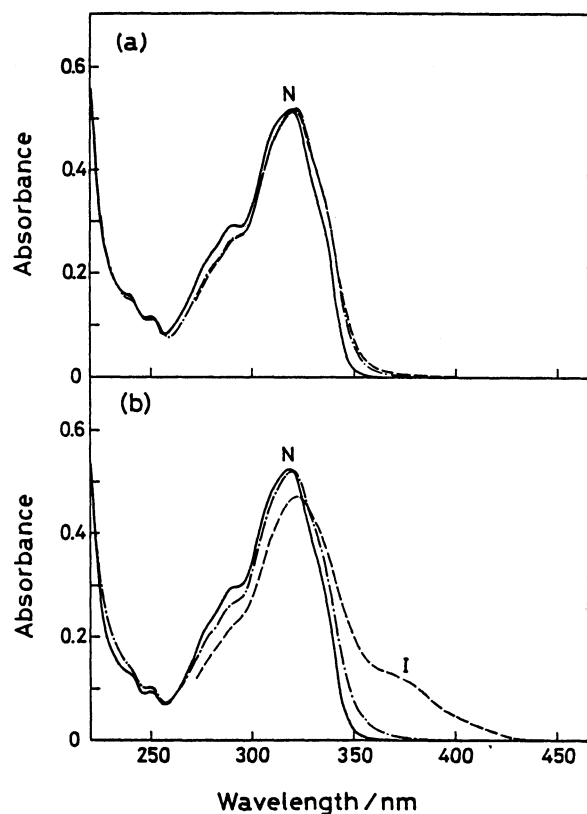
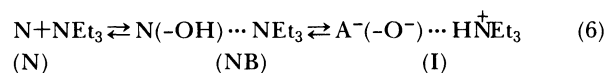


Fig. 6. UV absorption spectra of 7H4MC in dioxane (a) and in  $\text{CH}_3\text{CN}$  (b) for the neutral (—), acidic (---), and basic (----) solutions at 20°C.

red shift as in dioxane was observed in the acidic  $\text{CH}_3\text{CN}$  (Fig. 6(b)). Because of the very low  $D$  of dioxane, it is presumed that the acid-base complexes between the fluorophore and the additives, described as  $\text{N}(>\text{CO}) \cdots \text{HClO}_4$  and  $\text{N}(-\text{OH}) \cdots \text{NEt}_3$ , are formed, where the substituents in the parentheses are concerned in the association and where the dots represent an attractive interaction such as the hydrogen bond; these ground-state complexes are indicated by NH and NB respectively. The absorption-peak wavelengths measured under various solvent conditions are given in Table 2. Evidently, 7-hydroxycoumarins can work

as both acid and base, because they have a proton-donating hydroxyl group and a proton-accepting carbonyl group. Nagakura and Baba<sup>16)</sup> found that the absorption spectra of 1:1 hydrogen bond complexes of phenols with suitable bases in nonhydroxylic solvents were shifted to longer wavelengths compared with the absorption spectra of the unbonded species; the shift was typically about  $500\text{ cm}^{-1}$ , which corresponds to ca. 4 nm in the wavelength region of the present interest. Although a stoichiometric complex has not clearly been affirmed in the case of 7-hydroxycoumarins, it is probable that the hydrogen-bond interaction determines the absorption shift in the nonhydroxylic solvents dissolving  $\text{HClO}_4$  and dissolving  $\text{NEt}_3$  (TEA). The shifts of the NH and NB bands amount to 1–7 nm, as may be seen from Table 2.

In the basic  $\text{CH}_3\text{CN}$ , a long-wavelength side band (350–450 nm) appeared in addition to the main band NB at ca. 322 nm (Fig. 6(b)). This peakless side band, indicated by I, was always accompanied by the NB absorption, and the entire spectral profile was not changed by the further addition of TEA up to  $2.4\text{ mol dm}^{-3}$ ; this is in contrast with the result in MeOH, which has a  $D$  value similar to that of  $\text{CH}_3\text{CN}$  (the “iso- $D$ -value” solvent), where the complete dissociation of 7-OH has been realized. Since the side band is commonly observed in **2a** and **2b**, but not in **1**, the most probable situation is that the ion pair between 7H4MC and TEA described as  $\text{A}^-(-\text{O}^-) \cdots \text{HNEt}_3^+$  is generated as a result of the proton transfer in the acid-base complex due to the larger ionizing power of the solvents. If the ion pair is a stabilized molecular complex, and if it contributes to the long-wavelength absorption, the following ground-state equilibria must be taken into account:



Rigorously speaking, the ion pair I is a representative of variously coupled pairs, including such solvent-separated ones as  $\text{A}^-(-\text{O}^-) \cdots (\text{solvent})_n \cdots \text{HNEt}_3^+$ ; such a

Table 2. Peak Positions of the Absorption and Fluorescence Spectra of 7H4MC in the Nonhydroxylic Solvents under Neutral, Acidic, and Basic Conditions at 20°C

| Solvent   | $D^{20}$                              | Absorption |      |      |                 | Fluorescence     |                   |                   |                  |
|-----------|---------------------------------------|------------|------|------|-----------------|------------------|-------------------|-------------------|------------------|
|           |                                       | N          | NH   | NB   | I <sup>b)</sup> | *N <sup>c)</sup> | *NH <sup>d)</sup> | *NB <sup>d)</sup> | *I <sup>e)</sup> |
| <b>1</b>  | Benzene                               | 2.3        | 319  | 320  | 326             | 372              | 426               | 410               |                  |
|           | Dioxane                               | 2.2        | 319  | 321  | 321             | 373              | 422               | 409               |                  |
|           | $\text{CH}_3\text{COOC}_2\text{H}_5$  | 6.0        | 319  | 321  | 320             | 373              | 418               | 414               |                  |
| <b>2a</b> | $\text{CHCl}_3$                       | 4.8        | 321  | 323  | 328             | ca. 380          | 376               | 413               | 423              |
|           | $\text{CH}_2\text{Cl}_2$              | 8.9        | 320  | 321  | 327             | ca. 380          | 376               | 413               | 427              |
| <b>2b</b> | $(\text{CH}_3)_2\text{CO}^{\text{a)}$ | 21.2       | <325 | <325 | <325            | ca. 380          | 374               | 420               | 426              |
|           | $\text{CH}_3\text{CN}$                | 36.1       | 318  | 320  | 322             | ca. 380          | 375               | 419               | 449              |

a) Because of the absorption due to the solvent, the absorption peak, possibly < 325 nm, was not precisely decided. b) The absorption tail (360–400 nm) on the longer-wavelength side of the NB band. c) Found by excitation at 320 nm. d) Found by excitation at 360 nm. e) Found by excitation at 410 nm.

dispersed nature in the separation of ions may be reason why the I absorption is broad and peakless. It will be shown later that the ion pair I is intimately correlated with the excited-state ion pair,  $\tilde{A}^+(-O^-) \cdots H\tilde{N}Et_3$ , i.e.,  $\tilde{I}$ . Since  $HClO_4$  usually forms an ion pair by itself, even in considerably inert solvents, it seems proper to state that the acid-base pairing between the fluorophore and  $HClO_4$  has the structure described by  $N(>CO) \cdots H^+ \cdot ClO_4^-$ . However, in contrast to the case of TEA, no distinct sign of the proton transfer from  $HClO_4$  to fluorophore could be found by absorption measurements in the nonhydroxylic solvents with  $[HClO_4]$  less than  $0.3 \text{ mol dm}^{-3}$ .

Now that the information on the ground states is fully known, the fluorescent behavior of 7H4MC is to be explored; the typical fluorescence spectra in dioxane and in  $CH_3CN$  under the neutral, basic, and acidic conditions are compared to each other in Fig. 7. The light illumination for the neutral solution was carried out at 320 nm, which excited the N state; this yielded the  $\tilde{N}$  fluorescence. For the acidic and basic solutions, they were illuminated at 360 nm, thus exciting the long-wavelength side of the acid-base-complex absorption (NH and NB) and yielding the  $\tilde{NH}$  and  $\tilde{NB}$  fluorescences respectively. Figure 8 schematically depicts the peak positions in **1**, **2a**, and **2b** under various solvent

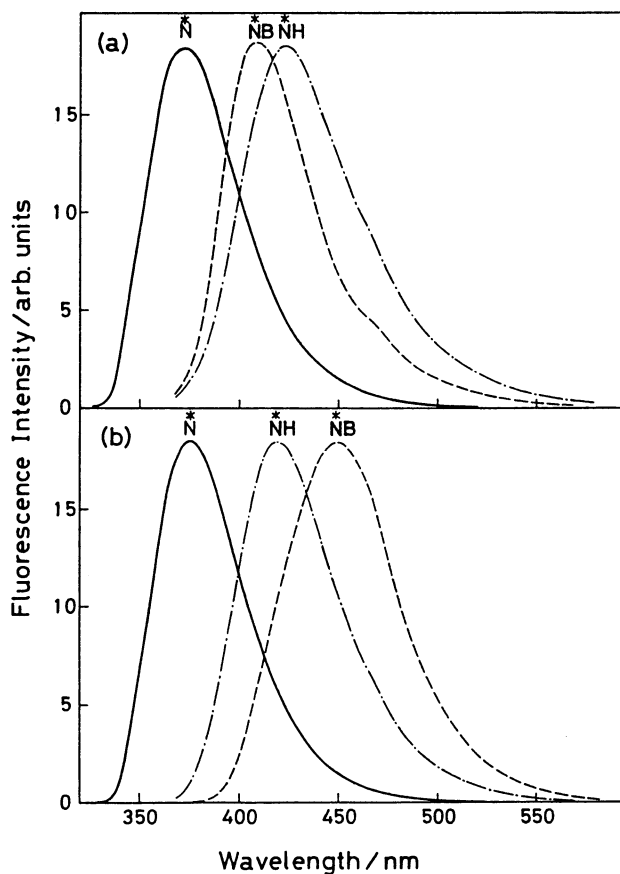


Fig. 7. Fluorescence spectra of 7H4MC in dioxane (a) and in  $CH_3CN$  (b) for the neutral (—), acidic (---), and basic (-·-·-) solutions at 20°C.

conditions, while Table 2 gives the results. The behavior of these bands can be clearly classified into two types. The fluorescence bands for the one are ordered in wavelengths  $\tilde{N} < \tilde{NB} < \tilde{NH}$  (Class 1); for the other, they are ordered  $\tilde{N} < \tilde{NH} < \tilde{NB}$  (Class 2). The solutions of benzene, dioxane, and ethyl acetate belong to Class 1 (Solvents **1**), while those of  $CHCl_3$ ,  $CH_2Cl_2$ , acetone, and  $CH_3CN$  belong to Class 2 (Solvents **2**), the latter being further divided into two groups (Solvents **2a** and **2b**). Here, judging from the energy position and the spectral shape, the  $\tilde{T}$  band, which was accompanied by the  $\tilde{N}$  band in the hydroxylic solvents, was not found in any nonhydroxylic solvent. The tautomerization of  $\tilde{N}$  to  $\tilde{T}$  may be supposed to be triggered only when the solvent has sufficient hydrogen-bonding ability and ionizing power, as in water and alcohols. This has been proved by the finding that the  $\tilde{T}$  band appears distinctly in the nonhydroxylic solvents upon the addition of a small amount of  $H_2O$ .

From Fig. 8 and Table 2, the following tendencies can, at least, be deduced: 1) The peak shift of the  $\tilde{N}$  band in each solvent class is small. 2) The  $\tilde{NH}$  band in **1** and **2a** is blue-shifted with an increase in  $D$ . 3) The  $\tilde{NB}$  band in **1** and **2a** is red-shifted with an increase in  $D$ . 4) By the selective excitation of I, new fluorescence bands ( $\tilde{I}$ ) appear around 450 nm in the basic solutions of **2a** and **2b** (dashed curves). Because the peak shift of the  $\tilde{N}$  fluorescence as well as the N absorption is small, the neutral species in the nonhydroxylic solvents has nonpolar structures in the excited and ground states. Considering that the deprotonation from acids and the protonation to bases in the nonhydroxylic solvents

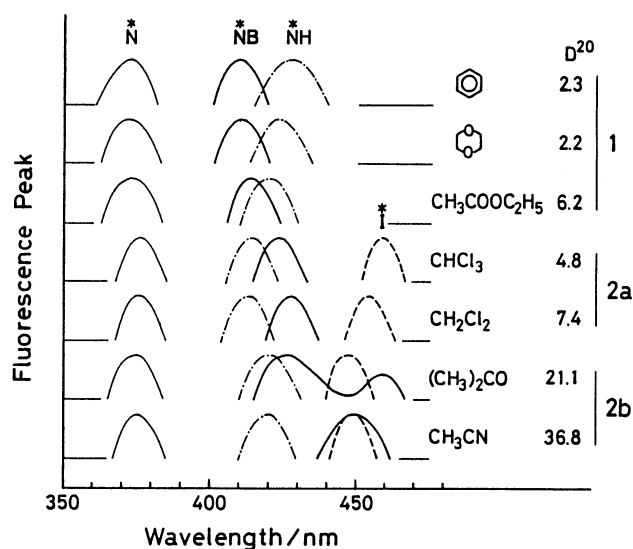


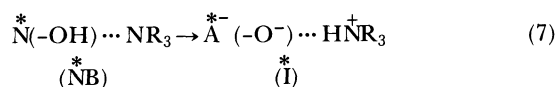
Fig. 8. Schematic drawings of the fluorescence peaks of 7H4MC in the nonhydroxylic solvents for the neutral (—), acidic (---), and basic (-·-·-) solutions excited at the main absorption band. The fluorescence peak shown by (---) was observed in the basic solutions of **2a** and **2b** excited at the long-wavelength absorption tail.



with lower  $D$  values are usually improbable, the  $^*\text{NH}$  and  $^*\text{NB}$  fluorescence in **1** and **2a** must originate from the excited-state acid-base complexes, analogous to the case in the ground state. Weller et al.<sup>17</sup> showed for several acid-base systems that a stronger hydrogen bond was possible in the excited state than in the ground state. Therefore, the larger red-shifts of the  $^*\text{NH}$  and  $^*\text{NB}$  bands from the  $^*\text{N}$  band, compared with those of the  $\text{NH}$  and  $\text{NB}$  bands from the  $\text{N}$  band, are reasonable (Table 2). As  $D$  is increased, the  $^*\text{NH}$  band systematically blue-shifts, but the  $^*\text{NB}$  band red-shifts throughout the solutions of **1** and **2a**, in contrast to the small shifts of the  $\text{NH}$  and  $\text{NB}$  bands. Confining ourselves to the case in **1** and **2a**, which have  $D$  values less than 10, the fluorophore complexed with  $\text{HClO}_4$  and with TEA is concluded to have a more polar structure in the excited state than in the ground state, although  $^*\text{NB}$  is stabilized and  $^*\text{NH}$  is destabilized by the increase in  $D$ . Such opposite tendencies result from the difference in the combining strengths of  $>\text{CO} \cdots \text{HClO}_4$  and  $-\text{OH} \cdots \text{NEt}_3$ ; the stabilization of the excited  $\pi$ -electron system due to the former is larger in **1**, while that due to the latter is larger in **2a**.

Several new features appear in the spectra when going from a low- $D$  solvent to a high- $D$  solvent. The

most prominent feature is that the fluorescence spectra in the basic solutions of **2a** and **2b** depend complicately on the excitation wavelength; some typical examples for  $\text{CHCl}_3$  and for acetone are shown in Fig. 9. Upon scanning the excitation towards longer wavelengths, the fluorescence spectra changed in shape and finally converged into a simple-shaped band at the excitation wavelength of 410 nm; this band is indicated by  $^*\text{I}$  in Figs. 8 and 9. Since 410 nm corresponds to the pure **I** absorption, the  $^*\text{I}$  fluorescence must result from the excited-state ion pair,  $^*\text{A}^-(\text{O}^-) \cdots \text{HNEt}_3$ . The ion-pair formation in the excited state has been confirmed by Weller et al. for a 2-naphthol-TEA system in methylcyclohexane.<sup>17</sup> Further, they have shown that the wavelength of the fluorescence increases with the promotion of ionization in the complex, in good accordance with the case of 7-hydroxycoumarins. In **2a**, the excitation of  $\text{NB}$  yields the pure  $^*\text{NB}$  state, while the excitation of **I** yields the pure  $^*\text{I}$  state; the critical transition of the excited state from  $^*\text{NB}$  to  $^*\text{I}$  upon a change in the excitation wavelength occurs at 400 nm, as may be seen from Fig. 9(a). This means that the potential barrier of the transformation between  $^*\text{NB}$  and  $^*\text{I}$  is large and that the proton transfer in the excited-state complex does not occur within its lifetime in the solutions of **2a**. In **2b**, on the other hand, the excitation of  $\text{NB}$  yields the long-wavelength component in addition to the  $^*\text{NB}$  contribution, whereas the excitation of **I** yields only the pure  $^*\text{I}$  state, as may be seen from Fig. 9(b). Such a feature comes from the large  $D$  values (more than 20) of **2b**. Probably, the potential barrier of the transformation between  $^*\text{NB}$  and  $^*\text{I}$  is small in **2b**, and so the following proton-transfer reaction becomes possible:



When  $^*\text{NB}$  is generated from  $\text{NB}$ , a mixture of  $^*\text{NB}$  and  $^*\text{I}$  is observed by the fluorescence measurements, as may be understood from Eq. 7. The proton-transfer equilibrium in the excited state between species like  $^*\text{NB}$  and  $^*\text{I}$  has been extensively studied by Weller et al. for the 2-naphthol-TEA system;<sup>17</sup> the results are analogous to the present case. The stabilization of  $^*\text{I}$  relative to  $^*\text{NB}$  depends, of course, on the solvent employed. In this connection, the Class 2 solvents have been divided into two groups at the earlier stage of the analysis; one is comprised of  $\text{CHCl}_3$  and  $\text{CH}_2\text{Cl}_2$  (**2a**, halogenated aliphatic solvents), and the other, of acetone and  $\text{CH}_3\text{CN}$  (**2b**, solvents with polar groups such as  $>\text{CO}$  and  $-\text{CN}$ ). From Table 2, the stabilization of the  $^*\text{I}$  state from the  $^*\text{NB}$  state in **2a** is pronounced, while that in **2b** is small or even absent. For the spectral change in **2b** with the excitation wavelength, the longer- and shorter-wavelength parts of the fluorescence band simultaneously decrease, while the center of the spec-

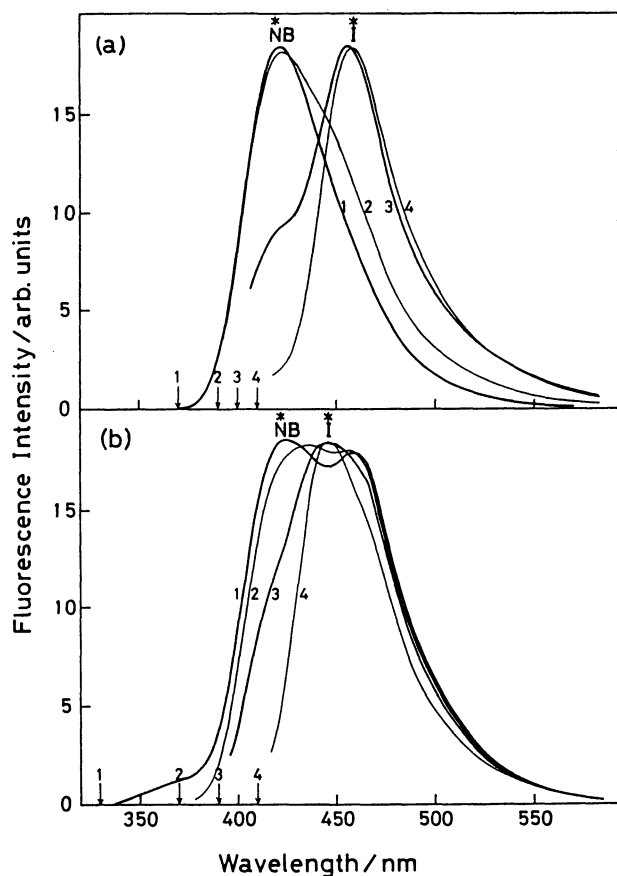


Fig. 9. Dependence of the fluorescence spectra of 7H4MC on the excitation wavelengths in the basic solutions of  $\text{CHCl}_3$  (a) and of acetone (b). The arrows numbered show the excitation wavelengths for the corresponding fluorescence spectra.

tra is roughly maintained (see Fig. 9(b)). Possibly, the **2a** solvents are suitable for the stabilization of the ion pair, while various types of ion pairs<sup>17)</sup> separated by such solvents as  $\bar{A}^-(-O^-) \cdots (\text{solvent})_n \cdots H\bar{N}Et_3$  will take part in the fluorescence in **2b**, because **2b** has the hydrogen-bonding ability through the  $>CO$  and  $-CN$  groups, though it is very small. The hydrogen-bonding ability of the solvents affects the potential barrier for the ion-pair formation, thus making the excited-state reaction of Eq. 7 possible. The complicated behavior of the fluorescence in **2b** is a manifestation of the complex nature of the acid-base complex and the ion pair.

It becomes clear that the hydrogen bond between the fluorophore and TEA persists through the nonhydroxylic solvents. This can be understood from the fact that the only effective hydrogen donor in the basic solution is the 7-OH group of the fluorophore. On the other hand,  $HClO_4$  is a rather unstable species as a hydrogen donor, especially in **2b**, due to the probabilities for self-ionization ( $H^+ClO_4^-$ ), proton donation to solvents ( $H^+ \cdots ClO_4^-$ ), and protonation of the fluorophore ( $\bar{C}^+(>COH^+) \cdots ClO_4^-$ ). Since the systematic blue shift of the  $\bar{N}H$  band is interrupted going from **2a** to **2b**, and since the peak position of  $\bar{N}H$  in **2b** is very close to that of  $\bar{C}^+$  in a hydroxylic solvent such as MeOH, a protonated fluorophore may be formed in the acidic solutions, i.e.,  $\bar{N}H \approx \bar{C}^+$  in **2b**. Similarly, the electronic state of  $\bar{I}$  in **2b** is thought to resemble that of  $\bar{A}^-$  of the hydroxylic solutions, judging from the good coincidence of their energy positions.

**Fluorescence Behavior in Mixtures of Hydroxylic Solvents.** The solvent polarity macroscopically represented by  $D$  is continuously changeable by using water-organic or organic-organic mixed solvents.<sup>8)</sup> Since the excited-state reactions of 7-hydroxycoumarins have been sensitively influenced by the solvent polarity, it seemed fruitful to investigate further the fluorescence change in water-alcohol and alcohol-alcohol mixtures as typical examples. Figure 10 shows the fluorescence spectra of 7HC in a "weakly acidic" solution ( $[HClO_4]=2 \times 10^{-5} \text{ mol dm}^{-3}$ ) and in an "acidic" solution ( $[HClO_4]=0.2-0.5 \text{ mol dm}^{-3}$ ) of  $H_2O$ -EtOH mixtures. Since the absorption was originated from  $\bar{N}$  under these conditions, the optical excitation was fixed at 338 nm, near the absorption peak. In the weakly acidic solution the  $\bar{N}$  and  $\bar{A}^-$  bands, as well as the weak contribution of the  $\bar{I}$  band, are observable, while in the acidic solution the  $\bar{N}$  and  $\bar{I}$  bands, separated considerably in wavelength, are observable. As the ethanol content of the solutions (EtOH wt%) is increased, the polarity and the hydrogen-bond strength decrease continuously; they very much influence the stability of the excited states and the mobility of proton in the solutions.<sup>18)</sup> From Fig. 10(a), the  $\bar{N}$  band in the weakly acidic solution enormously increases upon the increase in the EtOH wt%, while the  $\bar{A}^-$  band decreases. The weak  $\bar{I}$  contribution, noticed as a shoulder around 500 nm, seems to increase, though the quantitative separation of the overlapping  $\bar{A}^-$  and  $\bar{I}$  bands is difficult. The data can reasonably be explained if  $\bar{N}$  in the excited state

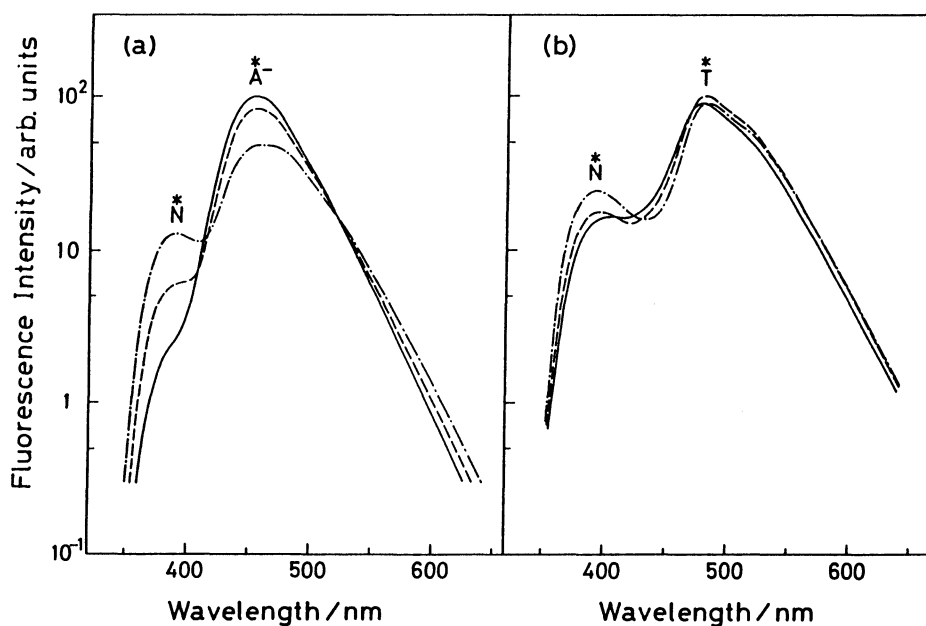


Fig. 10. Fluorescence spectra of 7HC in the  $H_2O$ -EtOH mixtures at 25°C. (a), the weakly acidic solution ( $[HClO_4]=2 \times 10^{-5} \text{ mol dm}^{-3}$ ) with the EtOH content: (—) 0 wt%, (---) 43 wt%, (-·-·-) 74 wt%. (b), the acidic solution ( $[HClO_4]=0.5 \text{ mol dm}^{-3}$ ) with the EtOH content: (—) 0 wt%, (---) 43 wt%, (-·-·-) 74 wt%.

becomes stabilized relative to  $\tilde{A}^*$  under lower polarity conditions. It is instructive to note that the ionizing power of EtOH for the N state is much lower than that of H<sub>2</sub>O, as has been shown in Fig. 2. Figure 11(a) shows the dependence of  $I^N/I_0^N$  on EtOH wt%, where  $I^N$  and  $I_0^N$  are the fluorescence intensities of the  $\tilde{N}$  band in the water-ethanol mixtures and in pure water respectively.

As for the acidic solution with 0.5 mol dm<sup>-3</sup> of HClO<sub>4</sub>, the change is not straightforward (Fig. 10(b)). As the EtOH wt% is increased, the  $\tilde{N}$  band increases and its peak position slightly blue-shifts, while the  $\tilde{T}$  band increases at first and then decreases, with the peak position red-shifted. In Fig 11(b), the dependence of  $I^N/I_0^N$  and  $(I^T/I_0^T)/(I^N/I_0^N)$  on EtOH wt% is plotted. Since the dependence of the fluorescence yield of each band on the solvent composition is not disregarded, it is difficult to know the precise reason for the curious behavior of the data at a low EtOH wt%. Nevertheless, because of the monotonic decrease in  $(I^T/I_0^T)/(I^N/I_0^N)$  at higher EtOH wt% values, the generation rate of the tautomeric form,  $\tilde{T}$ , will be basically determined by the solvent polarity, which is intimately concerned with the promotion of the tautomerization processes from  $\tilde{N}$  to  $\tilde{T}$ . In Fig. 5(a), log  $(I^T/I^N)$  vs. log  $D$  is plotted for the H<sub>2</sub>O-EtOH system under acidic conditions. The same results for the MeOH-EtOH and EtOH-*i*-PrOH system are shown by the representative points ( $\Delta$ ) in Figs. 5(a) and 5(b). The plots for H<sub>2</sub>O-EtOH deviate upwards from the straight dependence obtained earlier, while the plots for MeOH-EtOH and EtOH-*i*-PrOH follow the straight relationship. Obviously, H<sub>2</sub>O is in a special position among hydroxylic solvents, because it can contribute a stronger hydrogen bond, even in a mixture, than can the alcoholic mix-

tures with similar  $D$  values. Since the participation of H<sub>2</sub>O in the tautomerization of  $\tilde{N}$  to  $\tilde{T}$  has been shown to be most effective for the nondissociative pathway,<sup>4)</sup> it can naturally be understood that the  $I^T/I^N$  of H<sub>2</sub>O-EtOH system is larger than that of the alcoholic solvents (e.g., the value at MeOH in Fig. 5(a)). Further, H<sub>2</sub>O may form an ordered aggregation of the "ice-berg-like" structure around the fluorophore due to its manifold interactions, and the effective mobility of hydrogens may be raised compared with the value in the bulk solvent far from the fluorophore, where random structures of H<sub>2</sub>O and EtOH prevail in the thermal equilibrium.

**Solubilization into Micelles.** It has recently been found that 7-hydroxycoumarins, as well as 7-ethoxycoumarins,<sup>19)</sup> are solubilized into micelles formed in aqueous solutions of surfactants. When a surfactant with a concentration higher than the critical micelle concentration (cmc) is dissolved into the aqueous solutions of 7HC and 7H4MC, the fluorescent molecules are distributed between the micellar phase and the bulk-water phase. Such solubilization phenomena of fluorescers are detectable from the change in the fluorescence spectra as a function of the added concentration of surfactants ( $C_s$ ).<sup>19,20)</sup> Figure 12 shows the change in the fluorescence spectra of 7HC upon the addition of sodium dodecyl sulfate (SDS, cmc $\approx 8 \times 10^{-3}$  mol dm<sup>-3</sup>); Fig. 12(a) shows the spectra measured under the "weakly acidic" conditions ( $[HClO_4] = 3 \times 10^{-4}$  mol dm<sup>-3</sup>) at 25 °C, and Fig. 12(b), those measured under the "acidic" conditions ( $[HClO_4] = 0.5$  mol dm<sup>-3</sup>).

As for the weakly acidic solution, the  $\tilde{N}$  fluorescence increases and the  $\tilde{A}^*$  fluorescence decreases upon the addition of SDS; the  $\tilde{T}$  band seems to increase, though

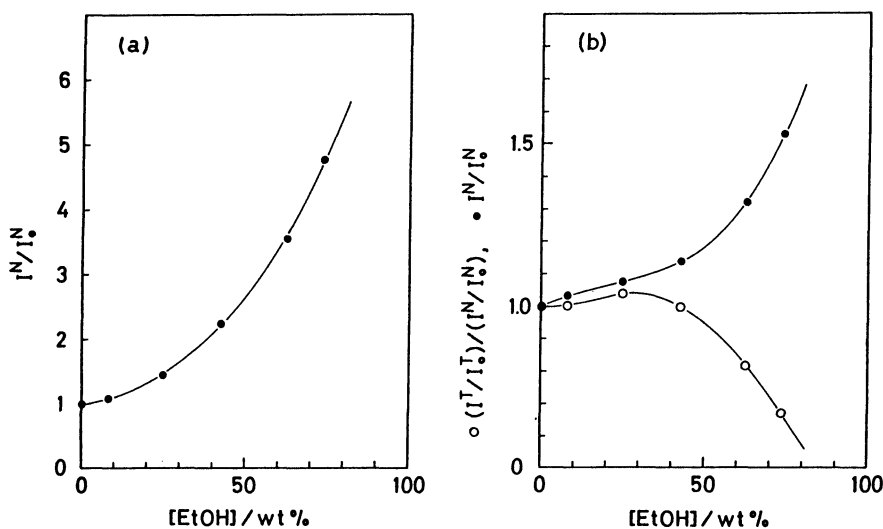


Fig. 11. Dependence of the relative fluorescence intensity of 7HC on the EtOH content of the H<sub>2</sub>O-EtOH mixtures at 25 °C. (a),  $I^N/I_0^N$  (●) vs. EtOH wt% in the weakly acidic solution; (b),  $I^N/I_0^N$  (●) and  $(I^T/I_0^T)/(I^N/I_0^N)$  (○) vs. EtOH wt% in the acidic solution.

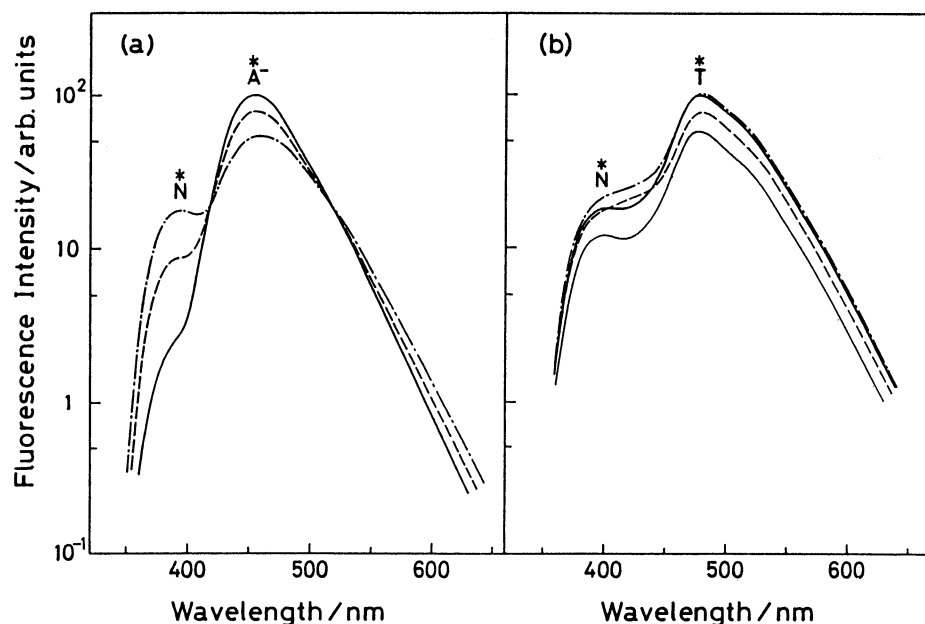


Fig. 12. Fluorescence spectra of 7HC in the aqueous micellar solutions of SDS at 25°C. (a), the weakly acidic solution ( $[\text{HClO}_4] = 3 \times 10^{-4}$ ) with the SDS concentration: (—)  $0 \text{ mol dm}^{-3}$ , (----)  $15 \times 10^{-3} \text{ mol dm}^{-3}$ , (---)  $50 \times 10^{-3} \text{ mol dm}^{-3}$ . (b), the acidic solution ( $[\text{HClO}_4] = 0.5 \text{ mol dm}^{-3}$ ) with the SDS concentration: (—)  $0 \text{ mol dm}^{-3}$ , (---)  $25 \times 10^{-3} \text{ mol dm}^{-3}$ , and the acidic solution ( $[\text{HCl}] = 0.5 \text{ mol dm}^{-3}$ ) with the SDS concentration: (—)  $0 \text{ mol dm}^{-3}$ , (----)  $25 \times 10^{-3} \text{ mol dm}^{-3}$ .

the quantitative separation of the overlapping  $\bar{A}^*$  and  $\bar{T}^*$  bands is difficult (Fig. 12(a)). Just as in the case of the  $\text{H}_2\text{O}$ -EtOH mixtures, the change is caused by the decrease in the microscopic polarity around the fluorophore solubilized into the micelle, for the interior of the micelle is hydrophobic and has a lower polarity

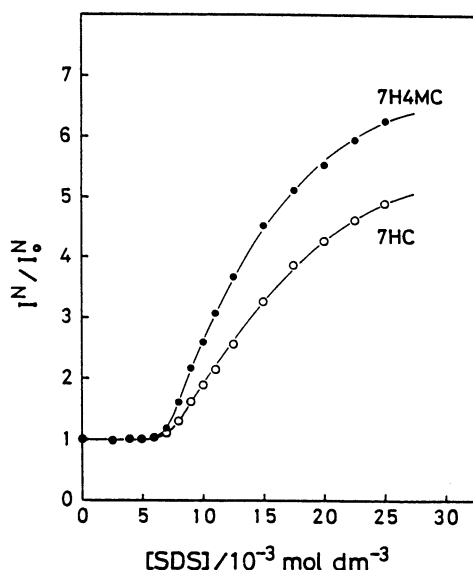


Fig. 13. Plots of the relative fluorescence intensity  $I^N/I_0^N$  vs.  $[\text{SDS}]$ , for 7HC and 7H4MC in the weakly acidic solution at 25°C. The fluorescence intensity was monitored at 380 nm for 7HC (○), and at 370 nm for 7H4MC (●), respectively.

than the bulk-water phase; the  $D$  value of the solubilized site within the micelle is between the values of aliphatic compounds (ca. 2) and of water (ca. 79).<sup>19)</sup> Therefore, the overall spectral change upon the addition of the surfactant is, in effect, similar to that in the case of  $\text{H}_2\text{O}$ -EtOH (Fig. 10(a)). Figure 13 shows that the relative fluorescence intensity  $I^N/I_0^N$  begins to increase abruptly when the SDS concentration reaches a value near the cmc. Because the fluorescence change is extremely sensitive to the micelle formation in the solution, even a small-sized pre-micellar aggregation of SDS can be detected as a subtle upward deflection of the plots around  $6 \times 10^{-3} \text{ mol dm}^{-3}$ . This value should be compared with the value of  $8 \times 10^{-3} \text{ mol dm}^{-3}$  determined by such macroscopic properties of the solution as the ionic conductance.<sup>21)</sup> The SDS concentrations from  $6 \times 10^{-3}$  to  $8 \times 10^{-3} \text{ mol dm}^{-3}$  are considered to form the transition region from rather unstable pre-micellar formation to stable micellar formation in the equilibrium state. It should be mentioned here that the micellization proceeds as a result of the stepwise-association reaction,  $D_{m-1} + S \rightleftharpoons D_m$  ( $S$  is the surfactant monomer,  $D_m$  is the micelle with  $m$  surfactants, and  $m \leq n$ , where  $n$  is the number of  $S$  in the stable micelle); strictly speaking, it is not a phase transition with a sharp variation in physical parameters. The change in the absorption spectra of several chromophores has usually been used as microscopic molecular probes for the micellization of surfactants.<sup>21)</sup> The fluorescence change which reflects such excited-state reactions as

$\text{N}^* \rightleftharpoons \text{A}^*$  is another candidate for an optically sensitive probe of microenvironments being formed in the aqueous micellar system.

As for the acidic solution with  $0.5 \text{ mol dm}^{-3}$  of  $\text{HClO}_4$ , the fluorescence change is less pronounced than that of the weakly acidic solution. A weak contribution from  $\text{C}^*$  appears between the  $\text{N}^*$  and  $\text{T}^*$  bands upon the addition of SDS, as can be noticed by the disappearance of the dip between them; the apparent increase in the fluorescence around the  $\text{N}^*$  band may be due to its contribution (Fig. 12 (b)). Since SDS is an anionic surfactant, cations are readily attached on the micelle surface and the  $[\text{H}^+]$  near the surface becomes higher than that in the bulk water. If the solubilization site of the fluorophore is not deep within the micelle,<sup>19,20)</sup> the  $\text{N}^*$  state generated from the solubilized  $\text{N}$  species by the light absorption will be protonated with  $\text{H}^+$  concentrated near the surface; consequently, the  $\text{C}^*$  fluorescence will appear. It is well-established that halide ions are able to quench the fluorescence from the excited species of coumarins.<sup>22-24)</sup> When the acid is altered from  $\text{HClO}_4$  to  $\text{HCl}$  in the same concentration, the fluorescence intensity is decreased as a whole (Fig. 12(b)). Because the  $\text{N}^*$ ,  $\text{A}^*$ , and  $\text{T}^*$  fluorescence were not quenched by  $\text{Cl}^-$  or  $\text{ClO}_4^-$  in the aqueous solution,<sup>11)</sup> the fluorescence quenching by the addition of  $\text{HCl}$  instead of  $\text{HClO}_4$  is attributable to the attractive interaction of  $\text{C}^*$  with  $\text{Cl}^-$ , which effectively induces the quenching. The  $\text{C}^*$  state generated by the excited-state reaction contributes, of course, to the tautomerization of  $\text{N}^*$  to  $\text{T}^*$  through the dissociative pathway and vice versa, although the  $\text{C}^*$  fluorescence is not detected to any extent in the solution without SDS. Therefore, both the  $\text{N}^*$  and  $\text{T}^*$  bands are decreased by the addition of  $\text{Cl}^-$  in the acidic solution. The total decay rate of  $\text{C}^*$  is composed of  $k_{41}$ ,  $k_{43}$ , and the fluorescence quenching rate,  $k_q$ , corresponding to the  $\text{C}^* + \text{Cl}^- \rightarrow \text{C} + \text{Cl}^-$  reaction; usually, their sum is larger than the generation rates of  $\text{C}^*$ ,  $k_{14}[\text{H}^+]$  and  $k_{34}[\text{H}^+]$ , whereas these are somewhat enhanced for the fluorophore solubilized within the anionic micelle, resulting in the appearance of the  $\text{C}^*$  fluorescence. Since anions such as  $\text{Cl}^-$  are kept away from the surface of the anionic micelle, contrary to the case with  $\text{H}^+$ ,<sup>11)</sup> the quenching by  $\text{Cl}^-$  against the solubilized fluorophore must be weakened by the addition of SDS. The fluorescence intensity of the  $\text{N}^*$  and  $\text{T}^*$  bands has been recovered in the presence of the micelle relative to the value in the absence of the micelle, as may be seen from Fig. 12(b). Consequently, the  $\text{N}^* \rightarrow \text{C}^* \rightarrow \text{T}^*$  tautomerization pathway has been clearly confirmed by means of the fluorescence quenching and the solubilization phenomenon.

### Conclusion

In order to explore systematically the complicated behavior of the fluorescence from the 7HC and

7H4MC solutions, solvents were divided into the two basic classes of hydroxylic and nonhydroxylic solvents, as popularly used in treating various chemical reactions in solutions. The fluorescence spectra in the hydroxylic solvents could be explained well by using the unified reaction model in the photo-excited states, which had been established by the study of the pH-dependent fluorescence in aqueous solutions. Especially, the fluorescence-intensity ratio between the neutral and tautomeric excited species in an acidic solution showed a remarkably straight relationship when  $\log(I^{\text{T}}/I^{\text{N}})$  was plotted against  $\log D$ . This resulted from the competitive reactions of the tautomerization between the dissociative and nondissociative processes.

The fluorescence spectra in the nonhydroxylic solvents differed greatly from those in the hydroxylic solvents, for the ionizing power and the hydrogen-bonding ability were small. The low polarity of the solvents resulted in the stable formation of hydrogen bond complexes or ion pairs between various acids and bases. From the fluorescent behavior, the nonhydroxylic solvents could be further classified into these three groups; the extremely inert solvents such as dioxane (1), the halogenated aliphatic solvents (2a), and the solvents with polar groups, such as  $>\text{CO}$  and  $-\text{CN}$  (2b).

The fluorescence in the water-alcohol and alcohol-alcohol mixtures and that in the aqueous micellar solutions were measured under various conditions. The parameter of  $\log D$  was well applicable to the alcoholic mixtures, although the aqueous alcohols behaved as stronger hydrogen-bonding solvents than had been expected. The solubilization of the fluorophore into the SDS micelle was detectable by the drastic change in the fluorescence spectra, and the possibility of the use of 7HC and 7H4MC as fluorescent probes of the microenvironment was pointed out.

The author gratefully acknowledges the financial support by the special research program on "Molecular Electronics" of the Ministry of International Trade and Industry, Agency of Industrial Science and Technology.

### References

- 1) O. S. Wolfbeis, E. Lippert, and H. Schwarz, *Ber. Bunsenges. Phys. Chem.*, **84**, 1115 (1980), and the references cited therein.
- 2) A. Diens, C. V. Shank, and R. L. Kohn, *IEEE J. Quantum Electron.*, **QE-9**, 833 (1973).
- 3) A. Bergman and J. Jortner, *J. Lumin.*, **6**, 390 (1973).
- 4) T. Moriya, *Bull. Chem. Soc. Jpn.*, **56**, 6 (1983).
- 5) T. Moriya and H. Anzai, *Bull. Electrotech. Lab.*, **46**, 431 (1982).
- 6) M. A. Paul and F. A. Long, *Chem. Rev.*, **57**, 1 (1957).
- 7) O. Bensaude, M. Dreyfus, G. Dodin, and J. E. Dubois, *J. Am. Chem. Soc.*, **99**, 4438 (1977).

- 8) Y. Y. Akhadow, "Dielectric Properties of Binary Solutions," Pergamon Press, Oxford (1980).
  - 9) J. Grzywacz and S. Taszner, *Z. Naturforsch.*, **33a**, 1307 (1978).
  - 10) N. Mataga and R. Kubota, "Molecular Interactions and Electronic Spectra," Marcel Dekker, New York (1970).
  - 11) T. Moriya, *Bull. Chem. Soc. Jpn.*, **61**, 753 (1988).
  - 12) J. G. Kirkwood, *J. Chem. Phys.*, **2**, 351 (1934).
  - 13) A. H. Fainberg and S. Winstein, *J. Am. Chem. Soc.*, **78**, 2770 (1956), and the references cited therein.
  - 14) H. Böhme and W. Schürhoff, *Chem. Ber.*, **84**, 28 (1951).
  - 15) R. G. Bates, "Determination of pH," John Wiley and Sons, New York (1973), Chap. 7.
  - 16) S. Nagakura and H. Baba, *J. Am. Chem. Soc.*, **74**, 5693 (1952).
  - 17) H. Beens, K. H. Grellmann, M. Gurr, and A. H. Weller, *Discuss. Faraday Soc.*, **39**, 183 (1965).
  - 18) M. Eigen and L. de Maeyer, "The Structure of Electrolytic Solutions," ed by W. J. Hammer, John Wiley and Sons, London (1959), p. 64.
  - 19) T. Moriya, *Bull. Electrotech. Lab.*, **50**, 1123 (1986).
  - 20) T. Moriya, *Bull. Chem. Soc. Jpn.*, **61**, 585 (1988).
  - 21) P. Mukerjee and K. J. Mysels, "Critical Micelle Concentrations of Aqueous Surfactant Systems," *Nat. Stand. Ref. Data Ser.*, **NBS 36** (1971).
  - 22) T. Moriya, *Bull. Chem. Soc. Jpn.*, **60**, 3855 (1987).
  - 23) T. Moriya, *Bull. Chem. Soc. Jpn.*, **57**, 1723 (1984).
  - 24) T. Moriya, *Bull. Chem. Soc. Jpn.*, **59**, 961 (1986).
-